THE HYDROSTATIC AND NONHYDROSTATIC LIMITS OF OCEAN MODELS AS TESTED ON BUOYANCY-DRIVEN FLOWS

S. Piacsek (1), P.Gallacher (1) and D.Dietrich (2)
(1) Oceanography Division, Naval Research Laboratory,
Stennis Space Center, MS, USA
(2) Acu-Systems, Inc, Albuquerque, NM, USA
piacsek@nrlssc.navy.mil /FAX +01-228-688-4759

The sensitivity of coastal ocean models to resolution, grid ratio and diffusivity is tested using simulations of a buoyantly driven internal bore. Three classes of models are compared: hydrostatic (H), fully nonhydrostatic (NH), and quasi-hydrostatic (QH). In the classic H approximation the vertical momentum equation reduces to a balance between the vertical pressure gradient and the buoyancy of the water. In the NH model the pressure is determined from a 3D elliptic equation that is derived by taking the divergence of the momentum equations. In the QH approximation the vertical velocity and pressure are determined by an iterative procedure, involving mass continuity and a diagnostic treatment of the vertical momentum equation. In this case only a 2D elliptic equation has to be solved, which is a great numerical advantage in 3D modeling.

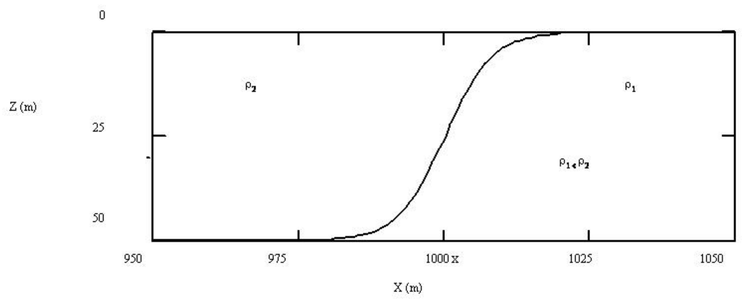

Figure 1. The initial conditions for the internal bore simulations. The channel is 2 km long and 50 m deep. The center 100 m of the channel is shown. The grid interval was 1.25m in the horizontal and 1m in the vertical. The time step was 0.5 seconds unless otherwise noted.

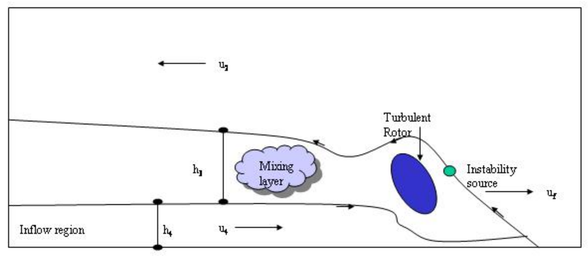

Figure 2. Schematic of frontal structure of an internal bore (After Marmorino and Trump [2000, Figure 1]). The front of a fully developed internal bore consists of a frontal head with a turbulent rotor, followed by a mixing layer, then a series of Kelvin Helmholtz (K-H) instabilities, and finally a train of lower amplitude internal waves.

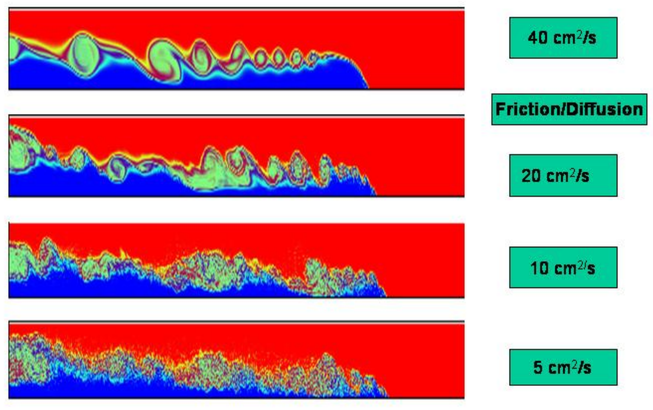

Figure 3. Friction/Diffusion Dependence of the NH-CAST Code
Already at A=40 cm^2/sec, fully developed K-H rollers are evident on the interface. As A is decreased, the rollers become more intense but also very noisy, until at A=5 cm^2/sec the mixing completely penetrates the advance half of the bore, with the "head" and edge losing their characteristics.

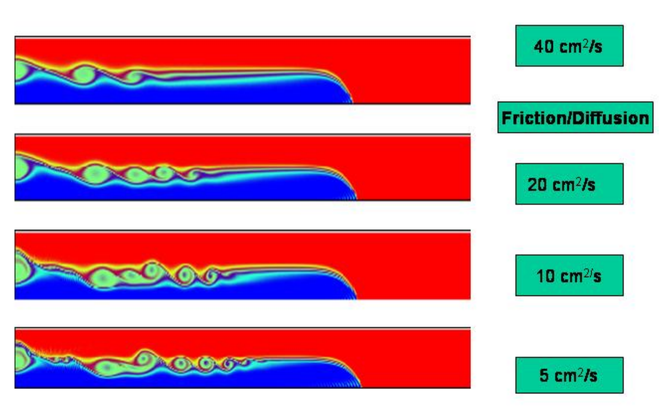

Figure 4. Friction Dependence of the QH-CAST Code.
For high values of the diffusion coefficients, the QH model develops only internal waves far upstream, whereas for low values, the proper K-H instabilities develop much closer to the leading edge of the bore. Compared to the NH model, the QH model is much less noisy but has no structure in the "head" region near the front.

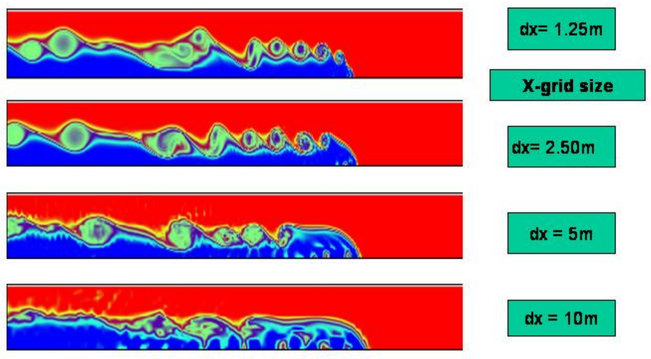

Figure 5. Grid Dependence of NH2D Code
The vertical grid remained at dz = 1m in all cases. As the ratio r = dx/dz increases from 1.25 to 10, the characteristics of the frontal head and of the interfacial K-H instabilities changes significantly. The frontal head becomes elongated, the K-H rotors decrease in number and intensity, and their onset occurs much further upstream from the frontal edge. At r = 10, the connectivity of the incoming cold fluid to the head is lost, unlike at r = 1.25.

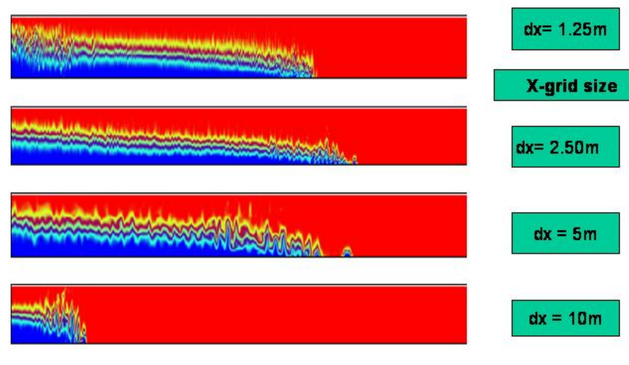

Figure 6. Grid Dependence of H-CAST Code.
As in Fig.5, the ratio r = dx/dz increases from 1.25 to 10. The most obvious characteristics of the hydrostatic simulations are the absence of the K-H rolls and a disintegration of the head. For A = 40 cm2/sec, strong short-wave noise appears for dx=1.25m, which grows in wavelength as dx -> 10m.

For horizontal to vertical grid ratios, $r = dx/dz < 4$, both the QH and the NH models exhibit nonhydrostatic characteristics. The propagation speed of the bore is approximately the same in the NH and QH models and is close to the theoretical inviscid speed. In the NH simulations the leading front of the bore, the rotor, and the mixing region behind the rotor are all well defined and agree with laboratory experiments and field measurements. Large amplitude internal waves and K-H instabilities are generated behind the mixing region. In contrast, for the same diffusivity values, the QH model has almost no rotor behind the bore edge and no mixing region. However, QH models do exhibit K-H instabilities on the plume-ambient fluid interface for small diffusivities, $A_h = A_z < 20$ cm^2/s. However, for large diffusivities A_h, $A_z > 80$ cm^2/s, both the rotor behind the bore front and the K-H instabilities disappear for all models.

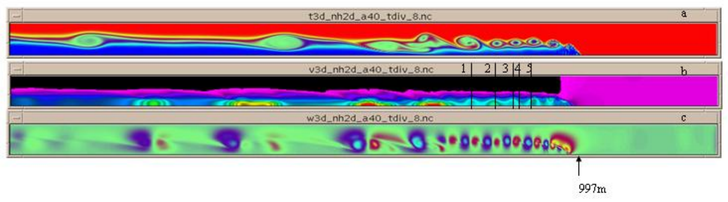

Figure 7. Temperature (a), horizontal velocity (b) and vertical velocity (c) of the nonhydrostatic internal bore after 100 minutes. Once the bore is fully developed the instabilities are forming about every 200 sec roughly 10-12m behind the leading edge of the front and about 10m from the bottom. These instabilities grow and move up and back from the their origin, over the rotor and into the mixing area. In the mixing area the K-H rolls are fully curled up at a distance of 45-50m behind the front and 15m above the bottom. The K-H rolls continue to propagate away from the rotor. Typically three fully developed K-H rolls exist behind the rotor. Then the K-H rolls coalesce causing intense mixing and forming a train of longer wavelength, smaller amplitude internal waves that propagate back away from the rotor.

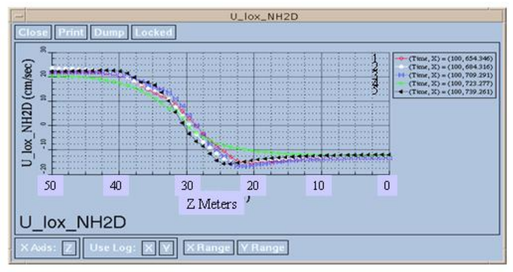

Figure 8. Profiles of horizontal velocity at the 5 locations marked in Figure 7. An inflow region is clearly defined in the bottom 10m between 40-50 m with an inflow velocity of about 20 cm/s. A mixing layer extends from about 40 m to 20-22 m. Above 10 m the counter current is approximately 13cm/s and essentially depth independent.

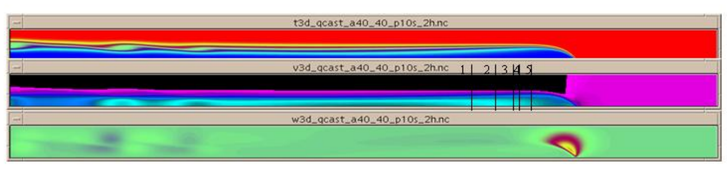

Figure 9. Temperature (a), horizontal velocity (b) and vertical velocity (c) of the internal bore after 100 minutes of the quasihydrostatic simulation. The viscosity is $0.004 m^2 s^{-1}$. In fact the solution looks more like the hydrostatic case than like the nonhydrostatic case. There is little evidence of internal waves, no overturning and no K-H instabilities. However, the propagation speed, 16.65cm/s, is nearly the same as in the nonhydrostatic case whereas the propagation speed in the hydrostatic case is much too small. Also the maximum horizontal, 23.9cm/s, and vertical, 10.8cm/s, velocities are closer the nonhydrostatic values than they are to the hydrostatic values.

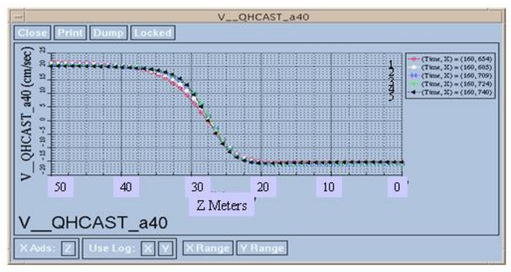

Figure 10. Profiles of horizontal velocity at the 5 locations marked in Figure 9. The inflow region (figure 8) is almost twice as wide as in the nonhydrostatic case and the velocity is slightly smaller. The mixing region is narrower than in the nonhydrostatic case, 10-12m versus 18-20m. The entire flow is more symmetric and the counter current is slightly greater, 15cm/s versus 13cm/s.

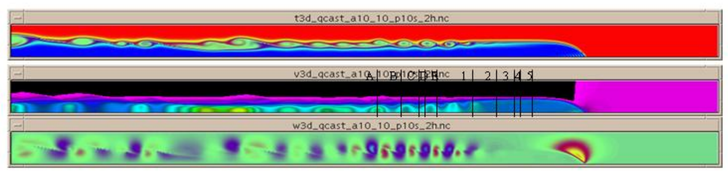

Figure 11. Temperature (a), horizontal velocity (b) and vertical velocity (c) of the internal bore after 100 minutes of the quasihydrostatic simulation. The viscosity is $0.001 m^2 s^{-1}$. The quasihydrostatic simulation exhibits much of the structure of nonhydrostatic simulation (Figure 7). Instabilities are generated, a mixing region exists, K-H rolls are generated behind the mixing region. These break down into internal waves with gradually decreasing amplitude and increasing wavelength as they propagate away from the front of the bore.

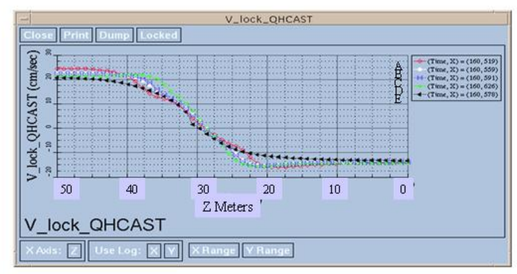

Figure 12. Profiles of horizontal velocity at the 5 locations (A-E) marked in Figure 11. when locations are chosen for the profiles based on the same criteria that was used in the nonhydrostatic case the results (Figure 11) are similar to the nonhydrostatic results. The criteria was to pick the first four maximums and the first minimum of the horizontal velocity. Then the results are: 1) the inflow region at the bottom is roughly 10m thick; 2) the mixing region is approximately 20m thick, about twice as large as the inflow region; 3) the inflow velocity is relatively uniform over the inflow region.

Conclusions:

In general, for horizontal to vertical grid ratios $r = dx/dz > 5$, both the nonhydrostatic (NH) and quasi-hydrostatic (QH) models behave like hydrostatic (H) models. For the H models the propagation speed is strongly a function of numerical method and grid resolution. For centered differencing schemes the propagation speed of the front in the H models was much less than in the QH and NH models and decreased with increasing r. With an upwind differencing scheme the propagation speeds of the H models almost matches those of the QH and NH models. However, the vertical velocity in the H models increases dramatically with decreasing dx, contrary to observations. This is due to the absence of inertial and friction terms in the w equation that normally oppose the acceleration of the vertical velocity; in the H models, w is obtained simply from the continuity equation.

The main findings are: (1) for the NH models - the bore front advances at the correct propagation speed, there is a rotor situated behind the front and a mixing region behind that; - the Froude number based on the front's advance and the internal wave speed of the two-layer fluid agrees closely with experiments (3-10%); - the full spectrum and amplitude of internal waves are generated; - K-H instabilities appear and grow on the large amplitude internal waves; (2) in the QH model - the bore has the same propagation speed as in the NH models; - however, there is almost no rotor action behind the bore edge; - the large amplitude internal wave train and the associated K-H instabilities are generated only for small diffusivity values (< 20 cm^2/sec) and with smaller amplitudes; (3) in the H models - the propagation speed of the bore is incorrect, - there is no rotor, no mixing region, and no large amplitude internal waves and - very little small amplitude internal waves.